Point Spread Function Reconstruction in Ground-based Astronomy

Raymond H. Chan
Department of Mathematics
The Chinese University of Hong Kong

Outline

1. Ground-based Astronomy
2. Models and Solution Methods
3. High-resolution Image Reconstruction

What is (gray-scale) image?

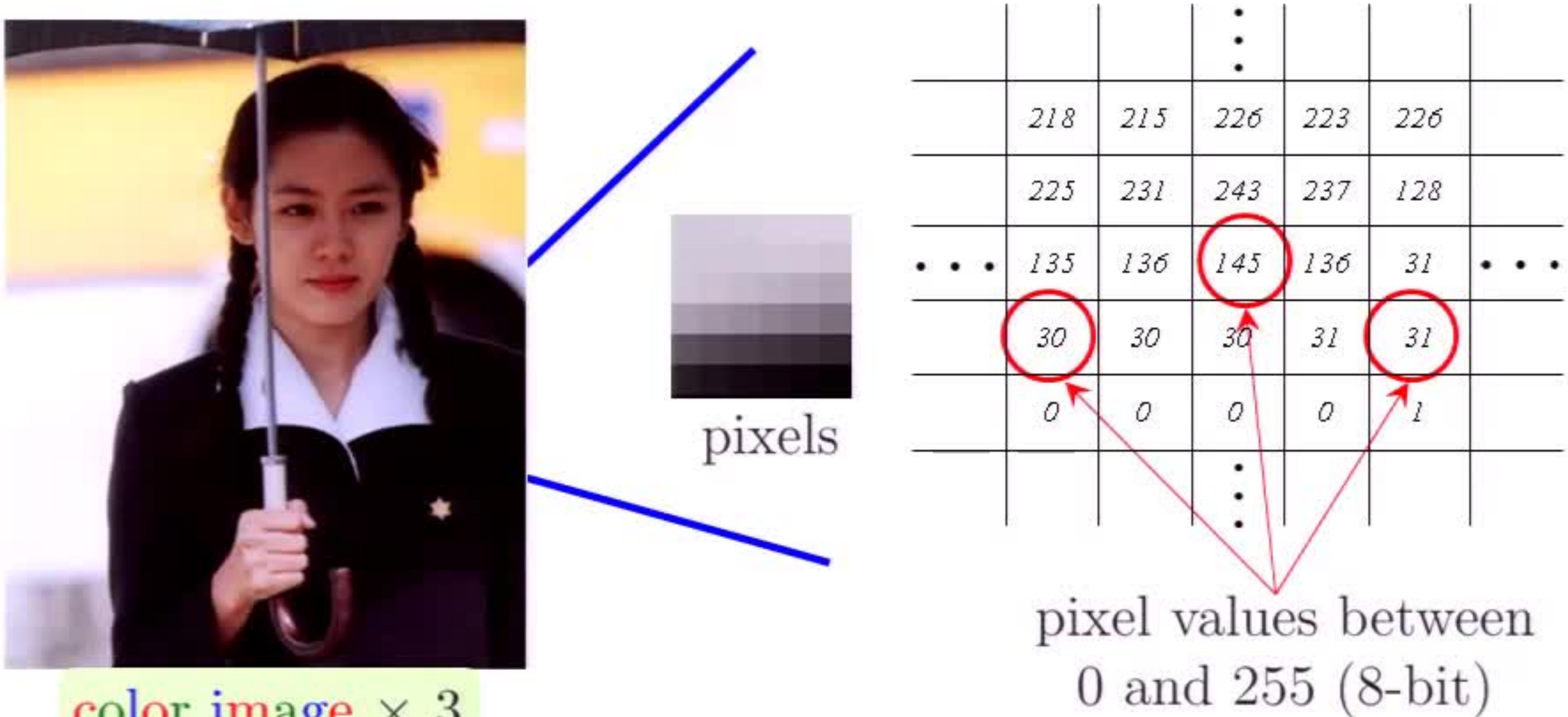

color image × 3

1000-by-1000 image = 1000-by-1000 matrix

concatenate into 1M-vector

Ground-Based Astronomy

true image
$f(x, y)$

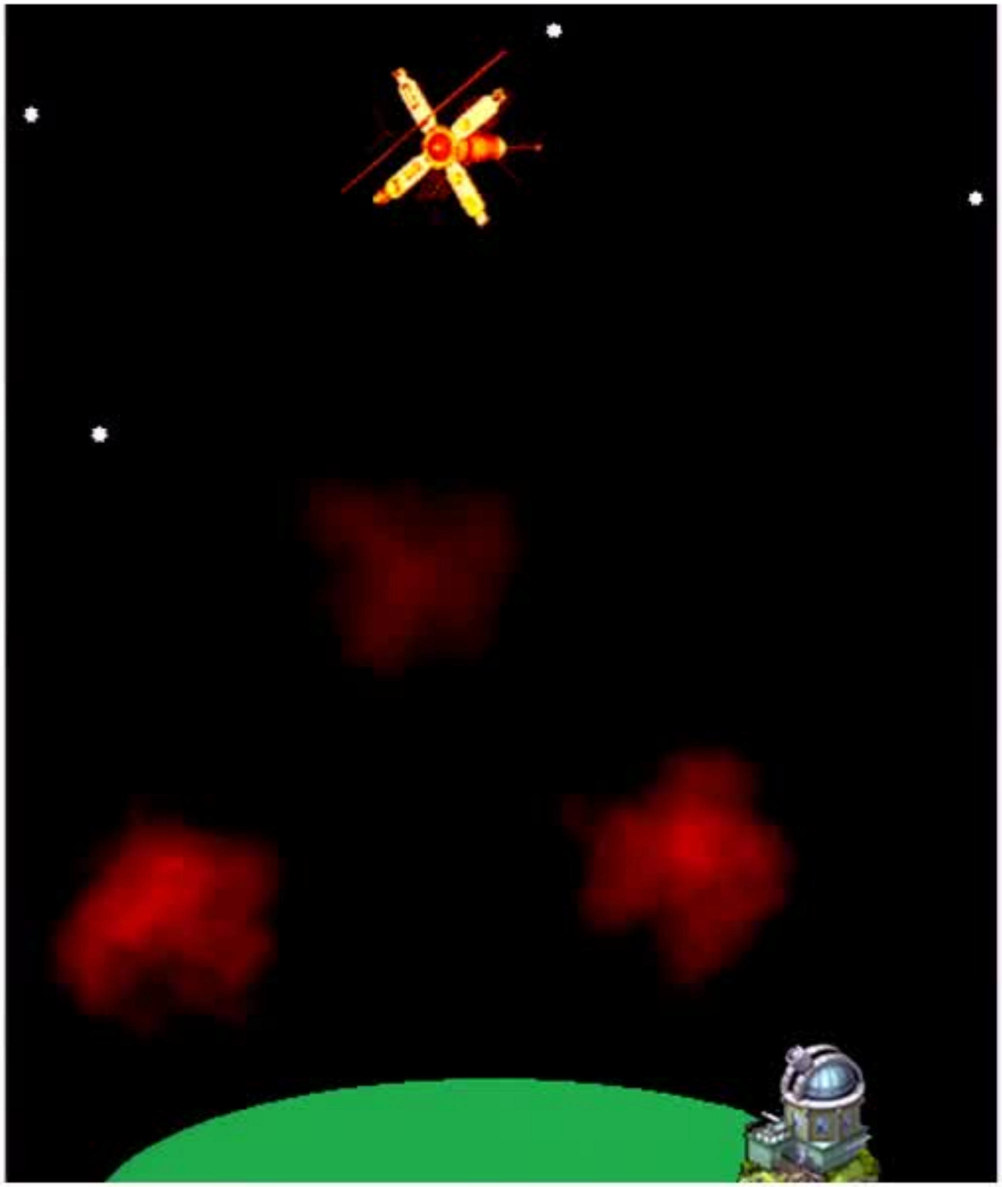

point spread function
$k(x, y)$

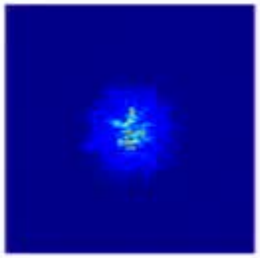

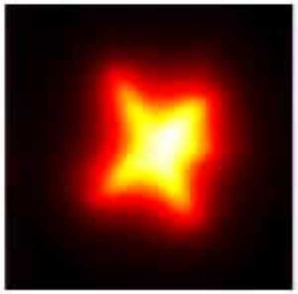

observed image
$g(x, y)$

Unknown Point Spread Functions

Some well-known approaches for getting $k(x, y)$:

- Blind-decovolution to simultaneously obtain $k(x, y)$ and $f(x, y)$:

$$g(x, y) = k^{(i+\frac{1}{2})}(x, y) * f^{(i)}(x, y) + n(x, y),\ i = 1, 2 \dots$$

[T. Chan & Wong IEEE TIP 98]

Unknown Point Spread Functions

Some well-known approaches for getting $k(x, y)$:

- ☐ Blind-decovolution to simultaneously obtain $k(x, y)$ and $f(x, y)$:

$$g(x, y) = k^{(i+\frac{1}{2})}(x, y) * f^{(i)}(x, y) + n(x, y),\ i = 1, 2 \ldots$$

[T. Chan & Wong IEEE TIP 98]

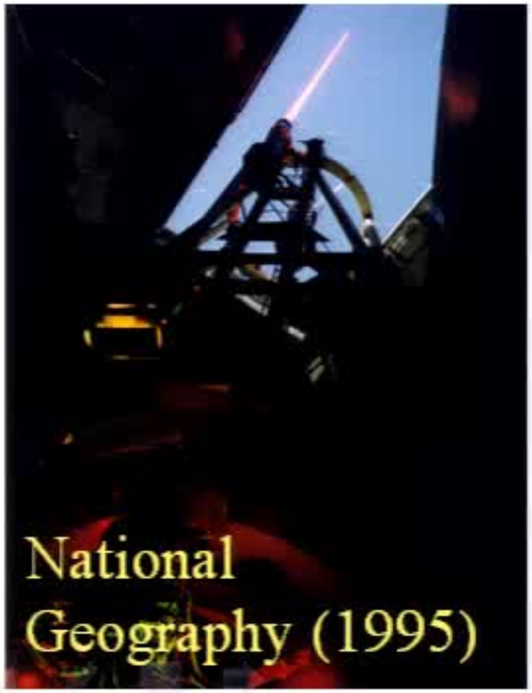

- ☐ Reconstruct $k(x, y)$ by some means (e.g. natural or artificial guide-star)

Ground-Based Astronomy

true image
$f(x,y)$

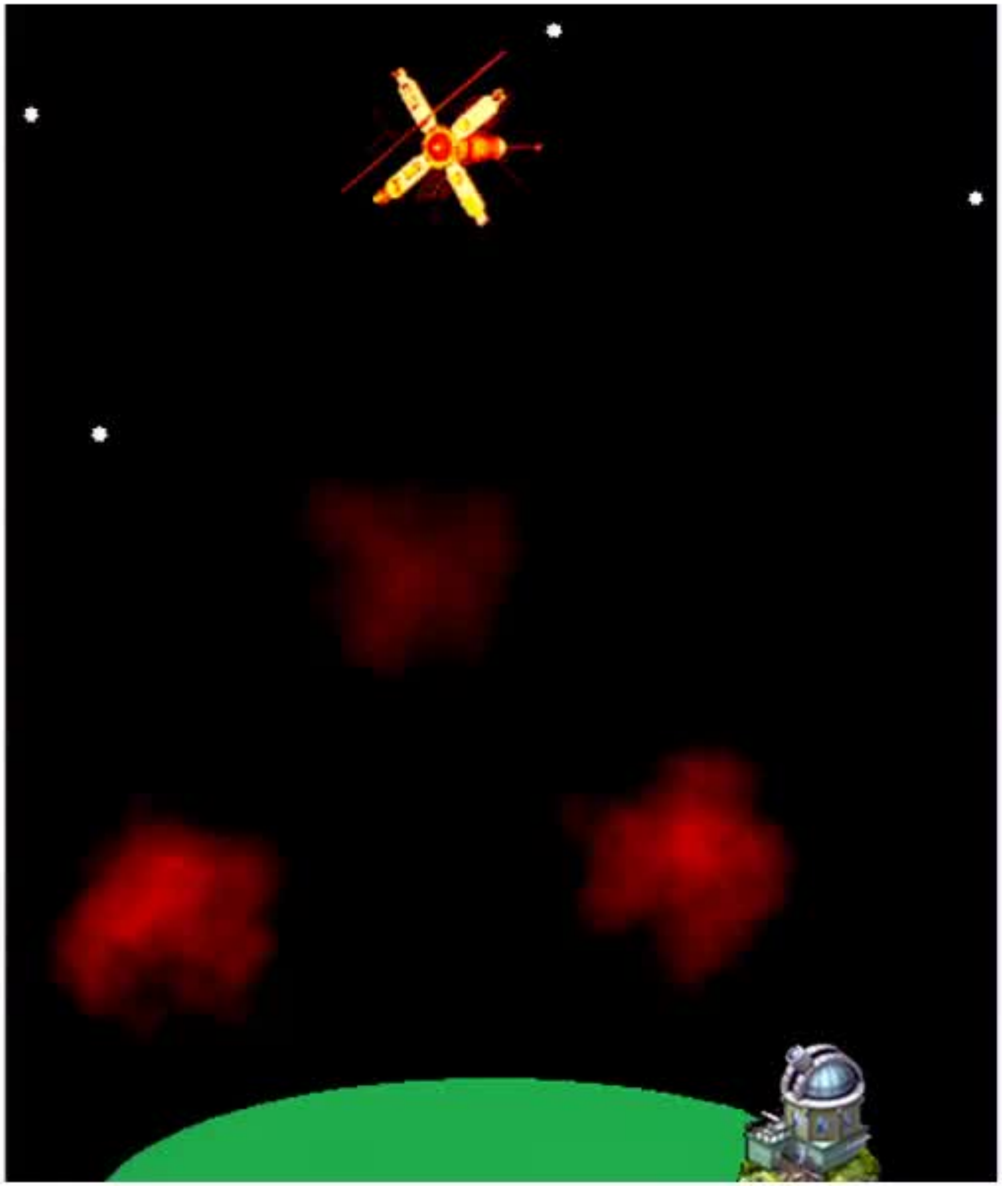

point spread function
$k(x,y)$

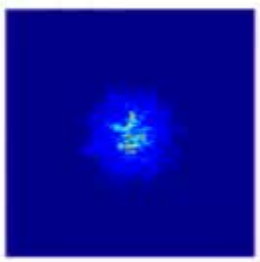

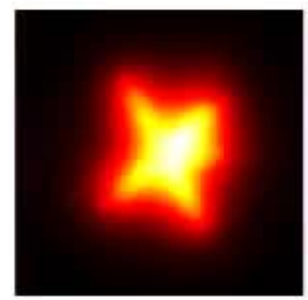

observed image
$g(x,y)$

Point-spread Function Reconstruction

Planar waves change across atmospheric turbulence

- $\phi(x, y)$: deviation from planarity is called phase error or phase

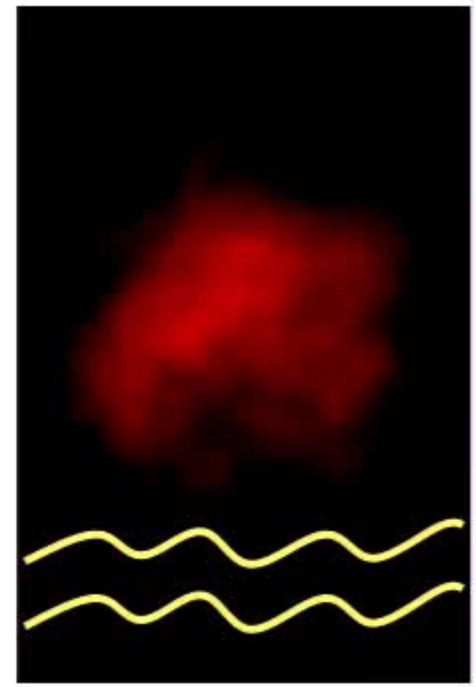

$\phi(x, y)$

Fourier optics model:

$$k(x, y) = \left| \mathcal{F}^{-1} \left\{ W(x, y) e^{i\phi(x,y)} \right\} \right|^2$$

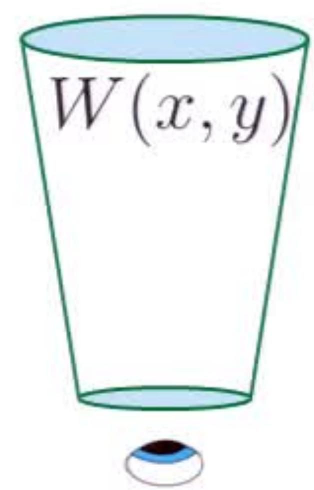

- $W(x, y)$: aperture of the telescope

- $\mathcal{F}$: Fourier transform

[Goodman 96, Bardsley SIMAX, 08]

Wavefront to Wavefront Gradient

Phase $\phi(x, y)$ cannot be directly measured, only its gradients by wavefront sensors:

phase ϕ

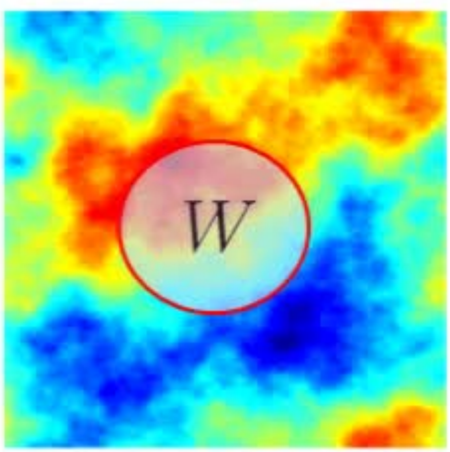

Wavefront to Wavefront Gradient

Phase $\phi(x, y)$ cannot be directly measured, only its gradients by wavefront sensors:

- ☐ $\mathbf{p}_x = D_x\phi(x, y)$: horizontal wavefront gradient
- ☐ $\mathbf{p}_y = D_y\phi(x, y)$: vertical wavefront gradient

D_i: 1st-order derivative operator modeling the sensor

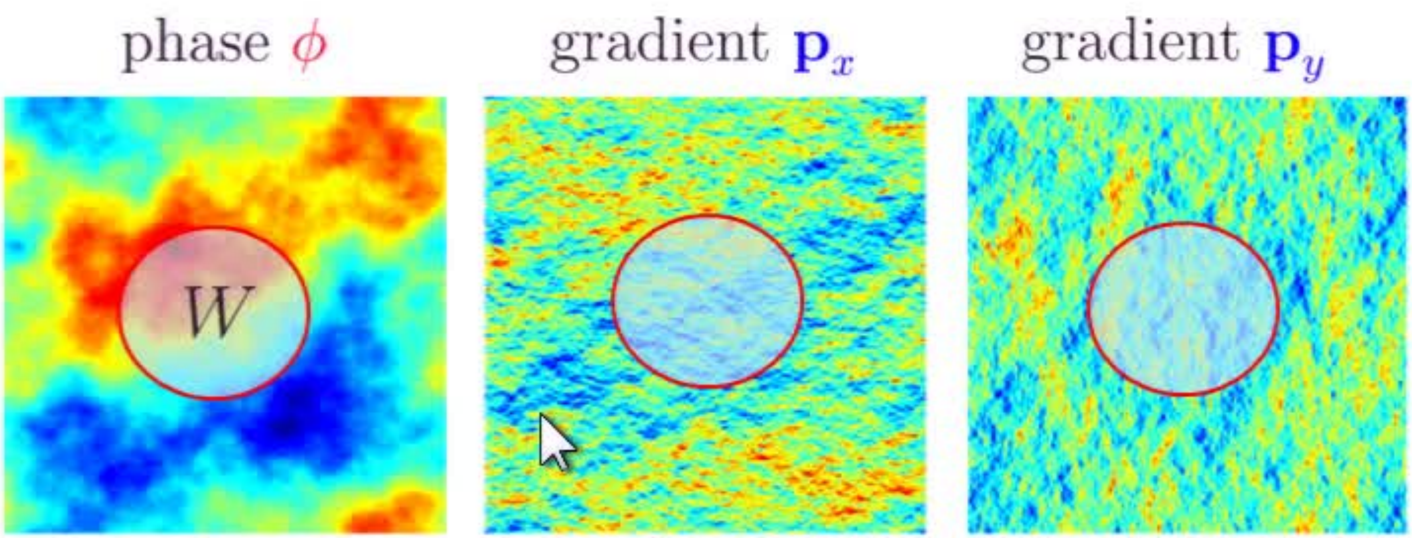

The Problem

- Wavefront sensors collect wavefront gradients $D_i\phi(x, y)$, not the phase $\phi(x, y)$
- $D_i\phi(x, y)$ are collected on coarse grids

Phase $\phi(x, y)$

$D_x\phi(x, y)$

- Not accurate to compute ϕ from $D_i\phi(x, y)$

The Aim

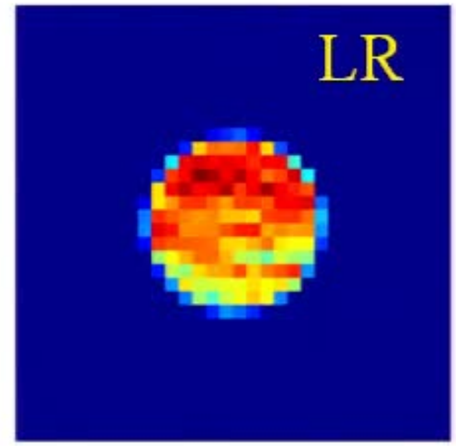

The Aim

- Use a sequences of low-resolution (LR) frames of wavefront gradients to obtain the high-resolution (HR) wavefront gradients $\mathbf{p}_i = D_i\phi(x, y)$
- From HR wavefront gradient $D_i\phi(x, y)$ reconstruct more accurate $\phi(x, y)$
- From $\phi(x, y)$ reconstruct $k(x, y)$
- Using $k(x, y)$, deblur $g(x, y)$ to get $f(x, y)$

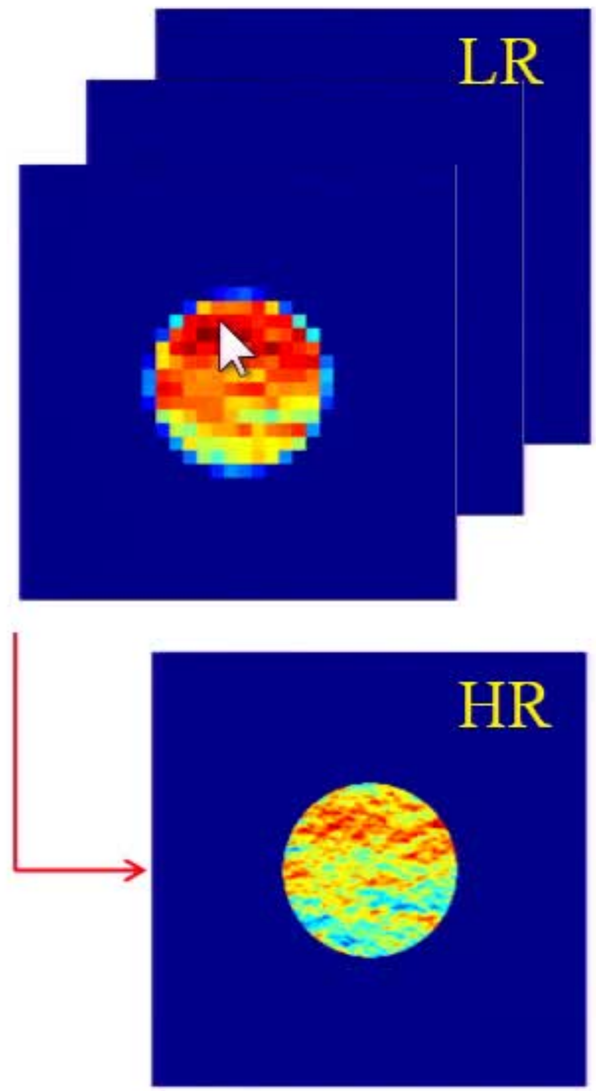

$\mathbf{p}_x$

Frozen Flow Hypothesis

Within a short time interval, phase does not change.

Move telescope to get a sequence of LR frames of wavefront gradients to reconstruct the HR wavefront gradients.

A LR wavefront gradients sensor

Frozen Flow Hypothesis

Within a short time interval, phase does not change.

Move telescope to get a sequence of LR frames of wavefront gradients to reconstruct the HR wavefront gradients.

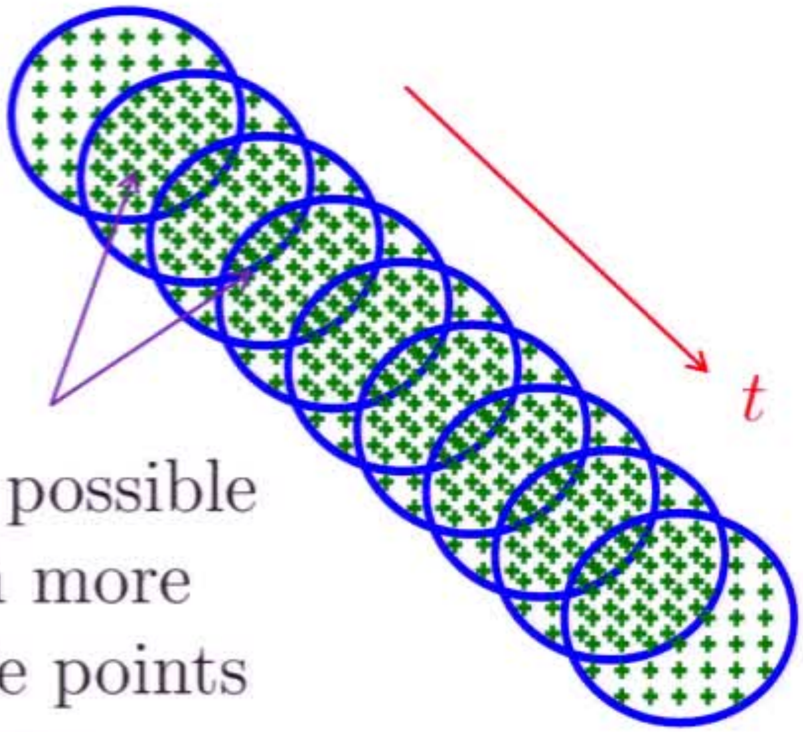

HR is possible with more sample points

A LR wavefront gradients sensor

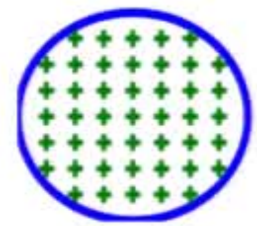

[Jefferies & Hart, 10]

Video Enhancement

A 352-by-288 video from a video recorder

20 to 30 frames/second

Bilinear interpolation from 1 frame

Video Enhancement

Reference frame

Improving resolution of LR reference frame

Video Enhancement

Reference frame

Improving resolution of LR reference frame

t

Video Enhancement

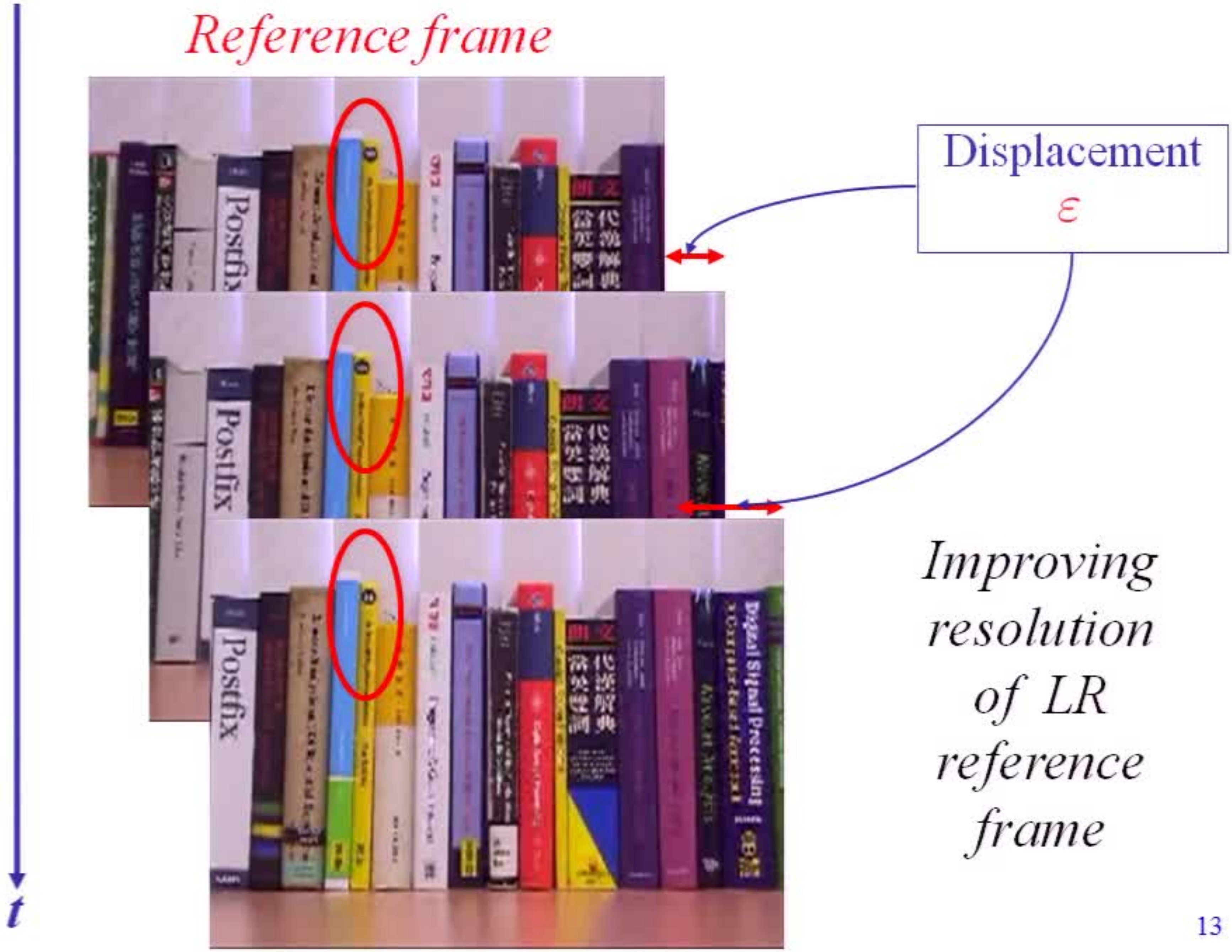

Improving resolution of LR reference frame

Video Enhancement

A 352-by-288 video
from a video recorder

Video Enhancement

A 352-by-288 video from a video recorder

Tight-frame method using 21 frames

[C., Shen, & Xia, ACHA 08]

More on this later in Part 3

Relation between HR and LR Gradients

$$\mathbf{q}_x^i = RWA_i\mathbf{p}_x + \mathbf{n}_x^i, \quad i = 1, 2, \cdots, m$$
$$\mathbf{q}_y^i = RWA_i\mathbf{p}_y + \mathbf{n}_y^i, \quad i = 1, 2, \cdots, m$$

- $\mathbf{p}_x$, $\mathbf{p}_y$: HR wavefront gradients
- $\mathbf{q}_x^i$, $\mathbf{q}_y^i$: sequences of LR wavefront gradients
- $\mathbf{n}_x^i$, $\mathbf{n}_y^i$: noise
- A_i: motion operator
- W: aperture operator
- R: down-sampling operator

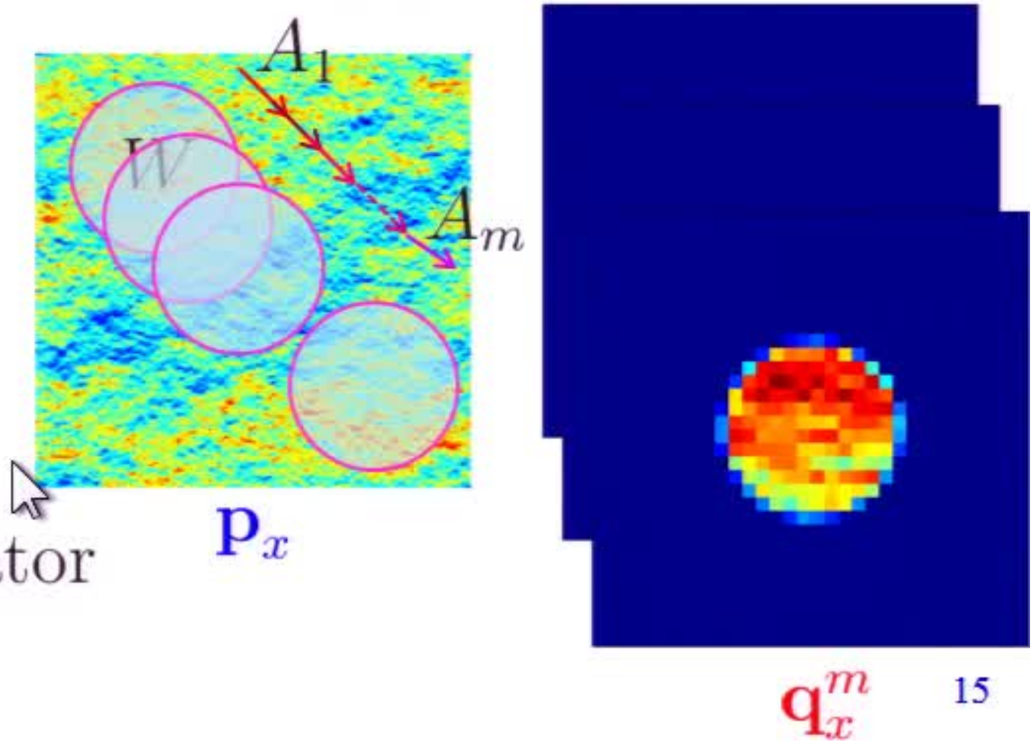

Tikhonov ℓ^2-ℓ^2 Model

[Nagy, Jefferies, & Chu, Maui Conf. 10, SISC 13]:

$$\min_{\mathbf{p}_x} \|\mathbf{p}_x\|_2^2 + \frac{\alpha}{2}\sum_{i=1}^{m} \left\| RWA_i\mathbf{p}_x - \mathbf{q}_x^i \right\|_2^2$$

$$\min_{\mathbf{p}_y} \|\mathbf{p}_y\|_2^2 + \frac{\alpha}{2}\sum_{i=1}^{m} \left\| RWA_i\mathbf{p}_y - \mathbf{q}_y^i \right\|_2^2$$

- linear solve with $\left[I + \alpha \sum_i (RWA_i)^T RWA_i\right]$
- $\|\mathbf{p}_x\|_2^2, \|\mathbf{p}_y\|_2^2 \approx \|\nabla\phi\|_2^2$
- may smooth the edges in ϕ

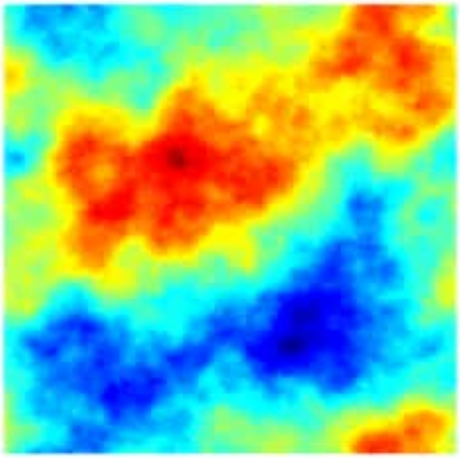

phase ϕ

Combined Model for the Phase

- Note that:

$$\begin{cases} \mathbf{q}_x^i = RW\,A_i D_x \phi + \mathbf{n}_x^i, \\ \mathbf{q}_y^i = RW\,A_i D_y \phi + \mathbf{n}_y^i, \end{cases} \quad i = 1, 2, \cdots, m.$$

- Treat ϕ as an "image" and regularize it:

$$\min_{\phi} \ \|C\phi\|_1 + \frac{\alpha}{2} \sum_{i=1}^{m} \left\| \begin{bmatrix} RW\,A_i D_x \\ RW\,A_i D_y \end{bmatrix} \phi - \begin{bmatrix} \mathbf{q}_x^i \\ \mathbf{q}_y^i \end{bmatrix} \right\|_2^2.$$

- Regularizer C can be TV, wavelet, tight-frame, fractional, ...

  [C., Yuan, & Zhang, Science China, 13]

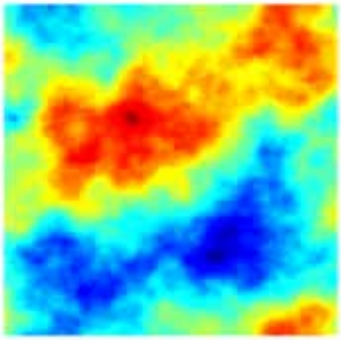

ϕ

Multi-layered Atmosphere

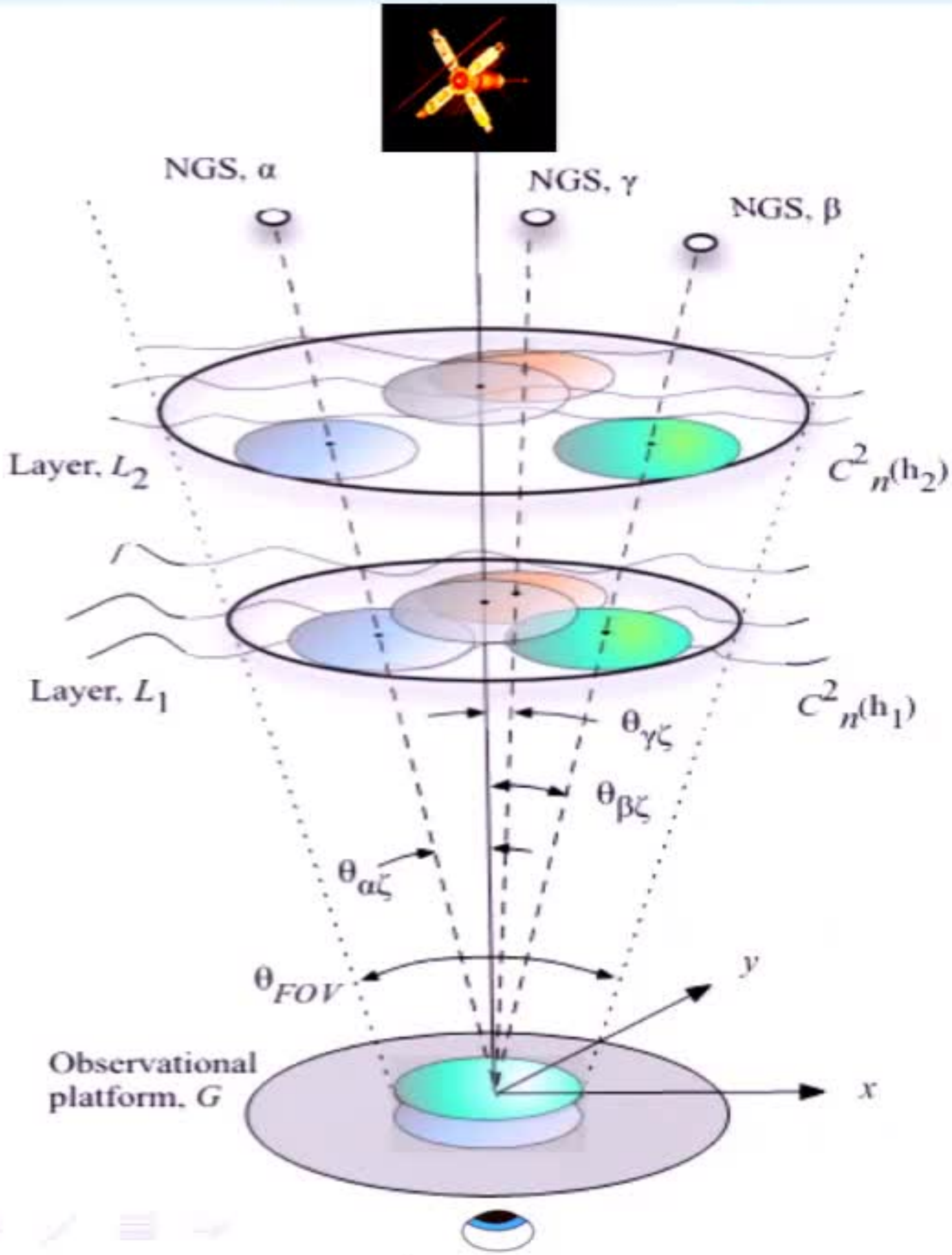

S.J. Weddell, "Optical wavefront prediction with reservoir computing".

Multi-layered Atmosphere

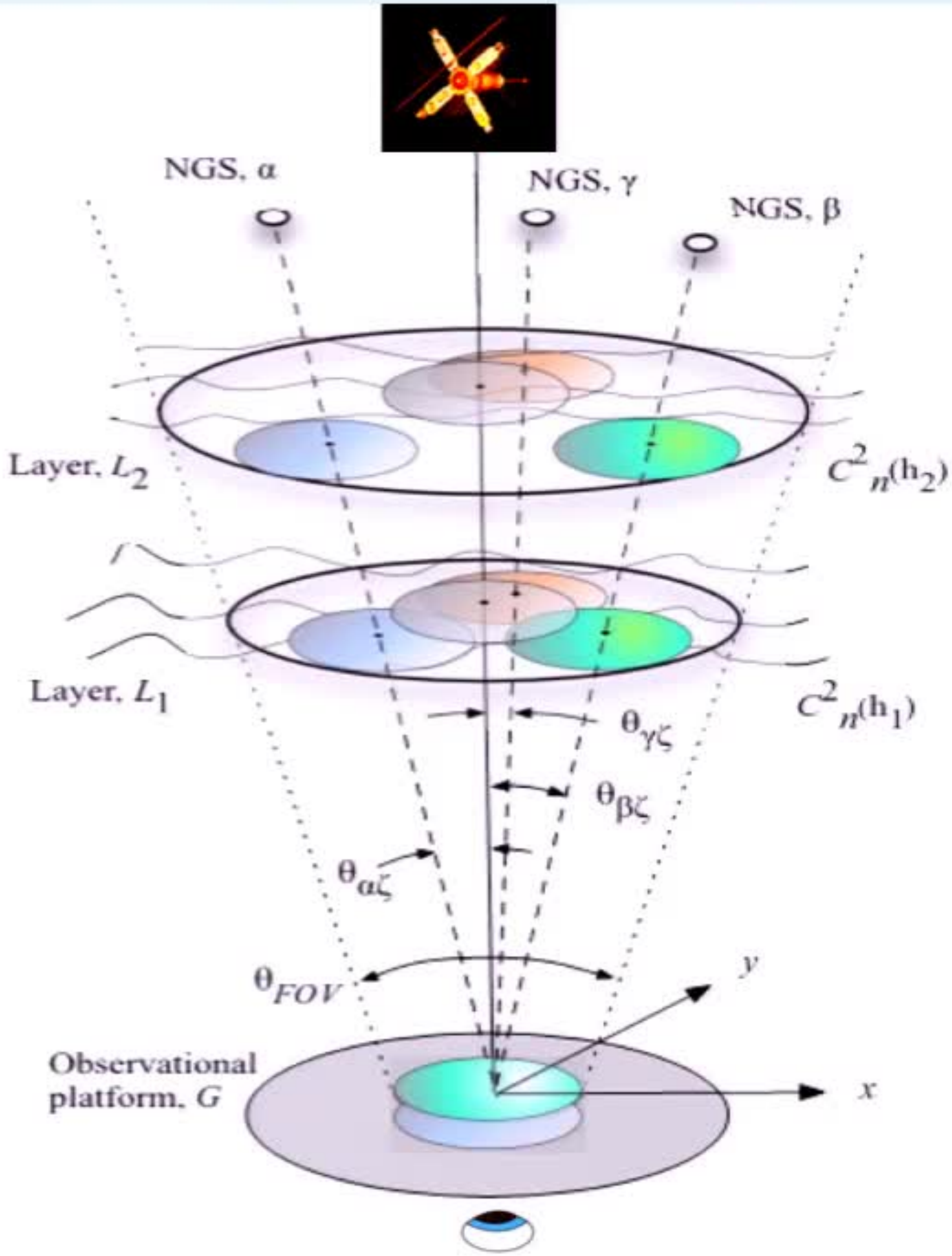

$\phi_2(x, y)$

$\phi_1(x, y)$

S.J. Weddell, "Optical wavefront prediction with reservoir computing".

Multi-layered Phase

One-layer ϕ

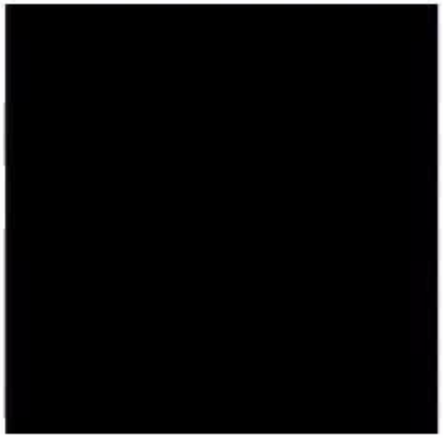

Multi-layer $\{\phi_l\}$

LR Horizontal $\mathbf{q}_x$

LR Horizontal $\mathbf{q}_x$

Experiment Setup

- generate true 256-by-256 ϕ [Nagy *et al.*, 10, 13]

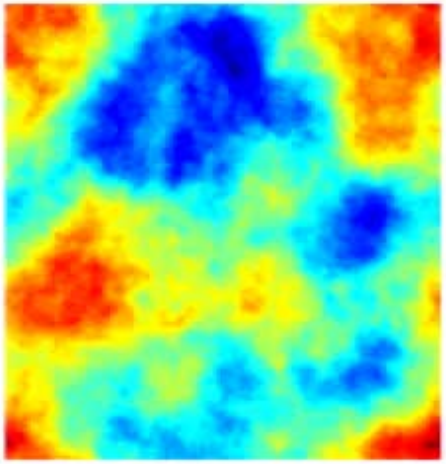

ϕ

Experiment Setup

- generate true 256-by-256 ϕ [Nagy *et al.*, 10, 13]
- generate HR $\mathbf{p}_x = D_x\phi$ and $\mathbf{p}_y = D_y\phi$
- generate LR $\mathbf{q}_j^i$ with 1% Gaussian noise by

$$\mathbf{q}_x^i = RWA_i\mathbf{p}_x + \mathbf{n}_x^i, \quad i = 1, 2, \cdots, m$$
$$\mathbf{q}_y^i = RWA_i\mathbf{p}_y + \mathbf{n}_y^i, \quad i = 1, 2, \cdots, m$$

- downsample by a factor of 4 (64-by-64 LR)
- use $m = 16$ frames

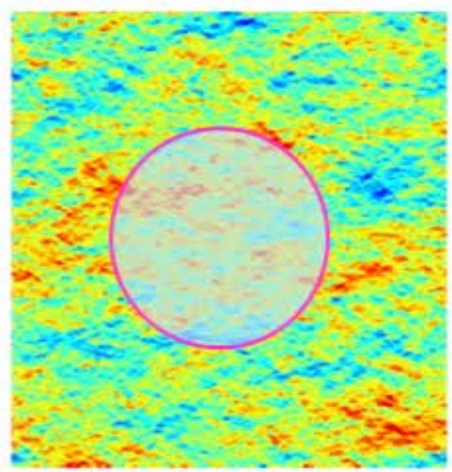

$\mathbf{p}_x$

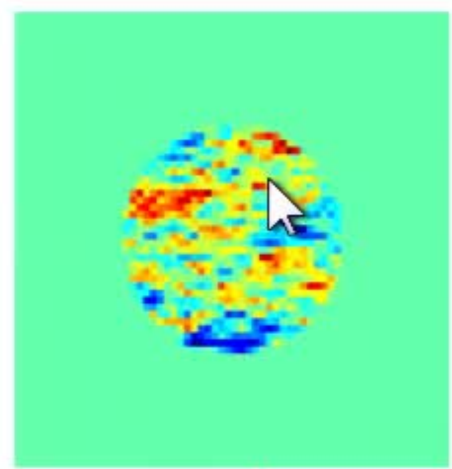

$\mathbf{q}_x^i$

Reconstructing the PSF

- Given $\{\mathbf{q}_x^i\}_{i=1}^m$ and $\{\mathbf{q}_y^i\}_{i=1}^m$, solve
  - $\min_{\mathbf{p}_x} \|\mathbf{p}_x\|_2^2 + \frac{\alpha}{2}\sum_{i=1}^m \|RWA_i\mathbf{p}_x - \mathbf{q}_x^i\|_2^2$
  - $\min_{\mathbf{p}_x} \|\mathbf{p}_x\|_1 + \frac{\alpha}{2}\sum_{i=1}^m \|RWA_i\mathbf{p}_x - \mathbf{q}_x^i\|_2^2$
  - $\min_{\phi} \|\nabla\phi\|_1 + \frac{\alpha}{2}\sum_{i=1}^{m} \left\| \begin{bmatrix} RWA_iD_x \\ RWA_iD_y \end{bmatrix} \phi - \begin{bmatrix} \mathbf{q}_x^i \\ \mathbf{q}_y^i \end{bmatrix} \right\|_2^2$
- Recover ϕ from $\mathbf{p}_x = D_x\phi$ and $\mathbf{p}_y = D_y\phi$
- Recover PSF from $k(x,y) = \left|\mathcal{F}^{-1}\left\{W(x,y)e^{i\phi(x,y)}\right\}\right|^2$
- Compare computed k_c with true k from true ϕ

PSF Error Comparison

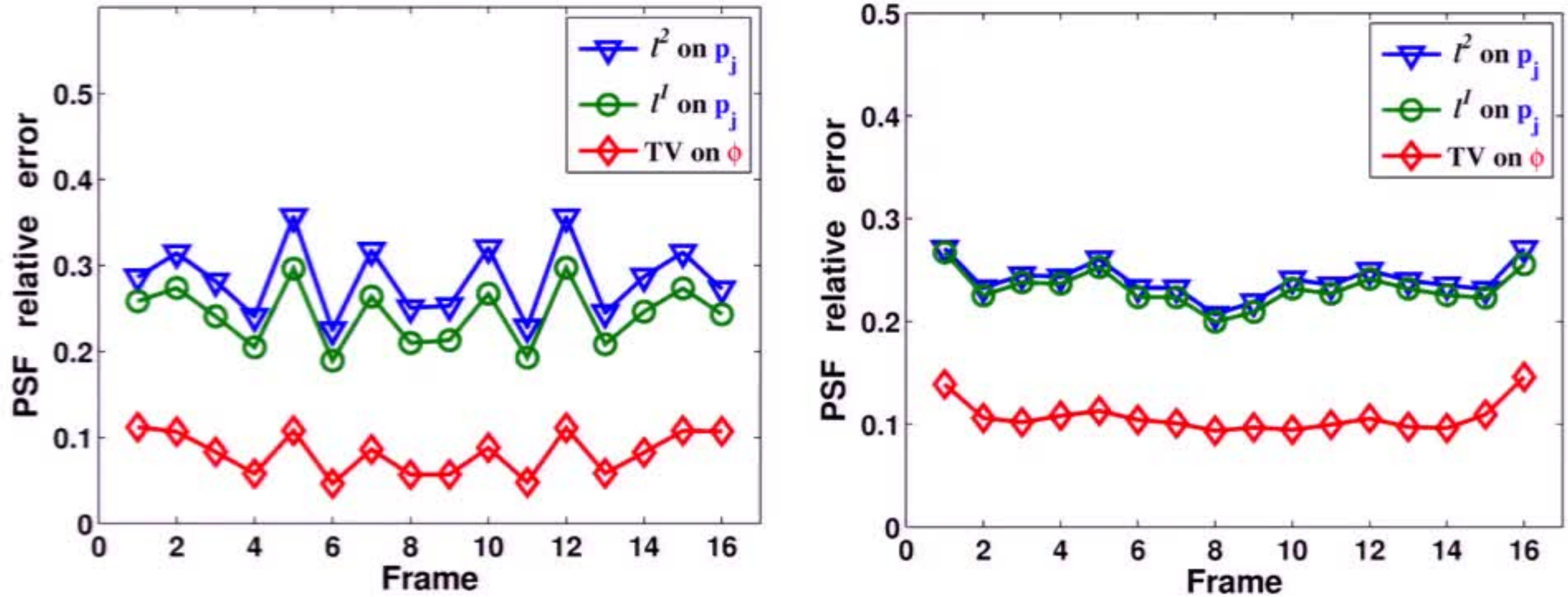

single-layer
seeing condition = 45

3-layer
seeing condition = 20

$\triangledown$: [Chu, Jefferies, & Nagy, SIAM J. Sci. Comput., 13]

$\circ$: [C., Yuan, & Zhang, J. Opt. Soc. Amer. A, 12]

$\diamond$: [C., Yuan, & Zhang, Science China A., 13]

How good is the Deblurring?

- Use true PSF $k(x,y)$ to generate blurred image:

$$g(x,y) = k(x,y) * f(x,y) + n(x,y)$$

with 1% Gaussian noise added.

$g(x,y)$

- In matrix terminology:

$$\mathbf{g} = K\mathbf{f} + \mathbf{n}$$

- Deblur $\mathbf{g}$ with computed PSF $k_c(x,y)$:

$$\min_{\mathbf{f}} \|\nabla \mathbf{f}\|_1 + \frac{\mu}{2}\|K_c\mathbf{f} - \mathbf{g}\|_2^2$$

Results for 1-Layer Case

1dB $\uparrow \approx$ 10% $\downarrow$ in relative error

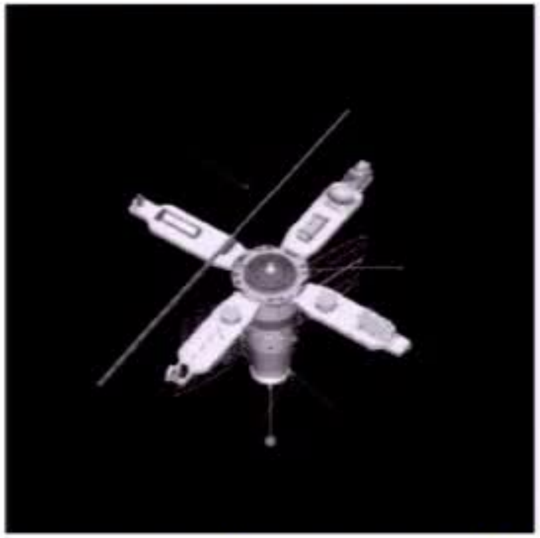

true image f

blurred image g

Results for 1-Layer Case

$1\text{dB} \uparrow \approx 10\% \downarrow$ in relative error

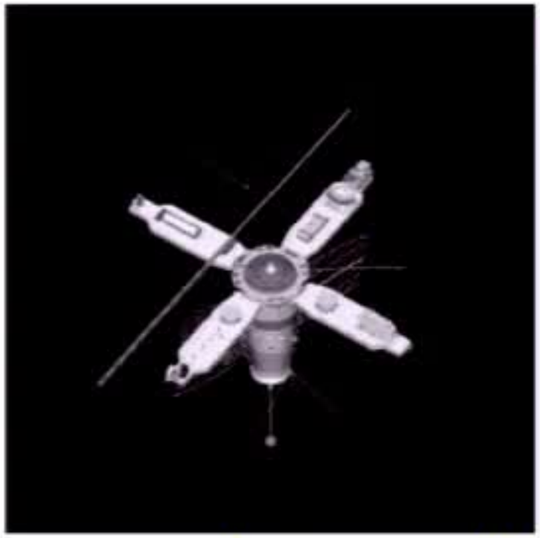

true image f

true psf

blurred image g

Results for 1-Layer Case

1dB $\uparrow \approx$ 10% $\downarrow$ in relative error

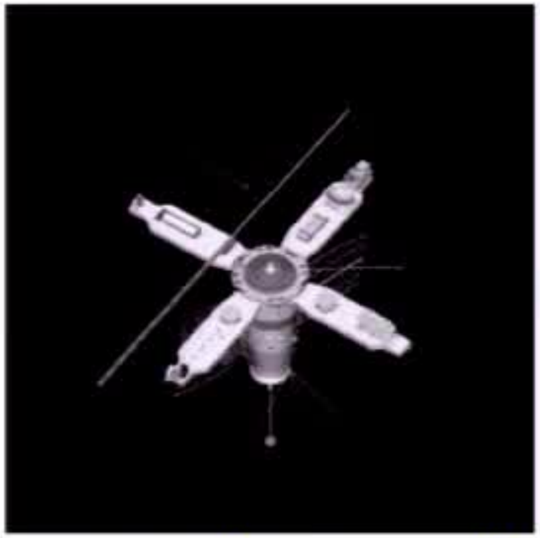

true image f

true psf

ℓ^2 on $\mathbf{p}_x, \mathbf{p}_y$

blurred image g

Results for 1-Layer Case

1dB $\uparrow \approx 10\% \downarrow$ in relative error

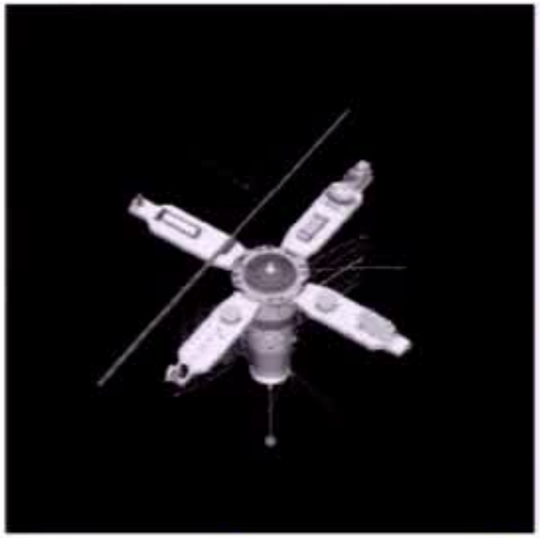

true image f

true psf

ℓ^2 on $\mathbf{p}_x, \mathbf{p}_y$

blurred image g

ℓ^1 on $\mathbf{p}_x, \mathbf{p}_y$

Results for 1-Layer Case

1dB $\uparrow \approx$ 10% $\downarrow$ in relative error

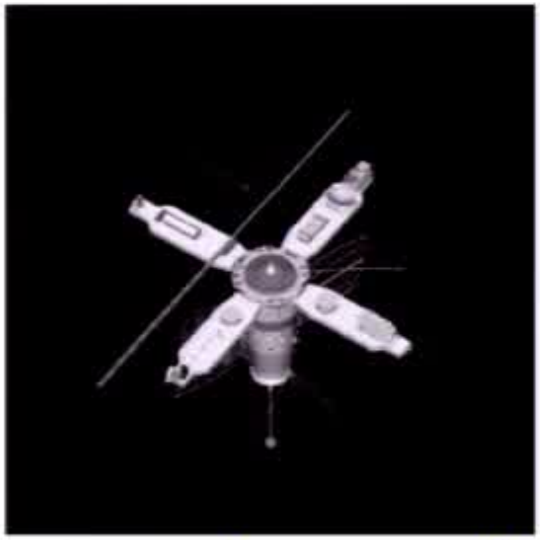

true image f

true psf

ℓ^2 on $\mathbf{p}_x, \mathbf{p}_y$

blurred image g

ℓ^1 on $\mathbf{p}_x, \mathbf{p}_y$

TV on ϕ

Results for 3-Layer Case

true image f

blurred image g

Results for 3-Layer Case

true image f

true psf

blurred image g

Results for 3-Layer Case

true image f

true psf

ℓ^2 on $\mathbf{p}_x, \mathbf{p}_y$

blurred image g

Results for 3-Layer Case

true image f

true psf

ℓ^2 on $\mathbf{p}_x, \mathbf{p}_y$

blurred image g

ℓ^1 on $\mathbf{p}_x, \mathbf{p}_y$

Results for 3-Layer Case

true image f

true psf

ℓ^2 on $\mathbf{p}_x, \mathbf{p}_y$

blurred image g

ℓ^1 on $\mathbf{p}_x, \mathbf{p}_y$

TV on ϕ

Classical Approach [Tsai & Huang, 84]

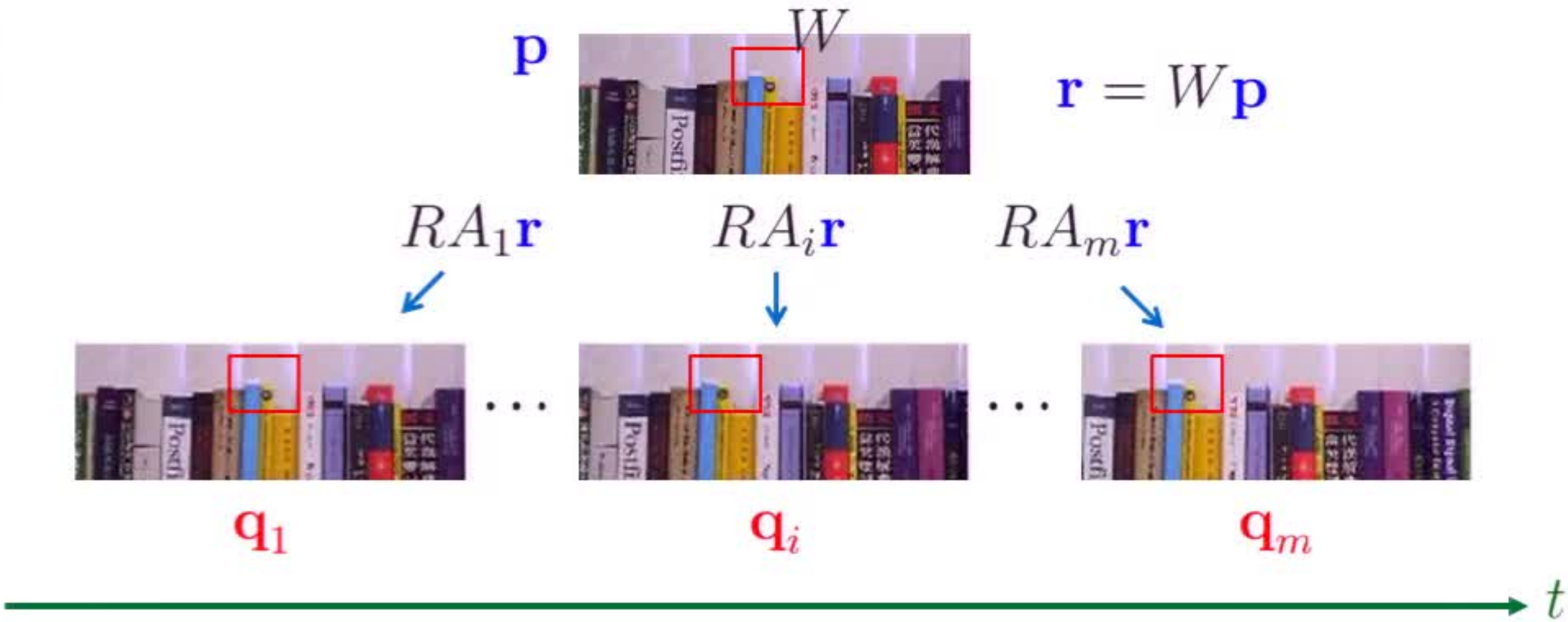

- ☐ $\mathbf{q}_i = RBA_i\mathbf{r} + \mathbf{n}_i, i = 1, \ldots, m$
- ☐ Solve, e.g.

$$\min_{\mathbf{r}} \|\nabla \mathbf{r}\|_1 + \frac{\alpha}{2}\sum_{i=1}^{m} \|RA_i\mathbf{r} - \mathbf{q}_i\|_2^2.$$

Low-rank Approach

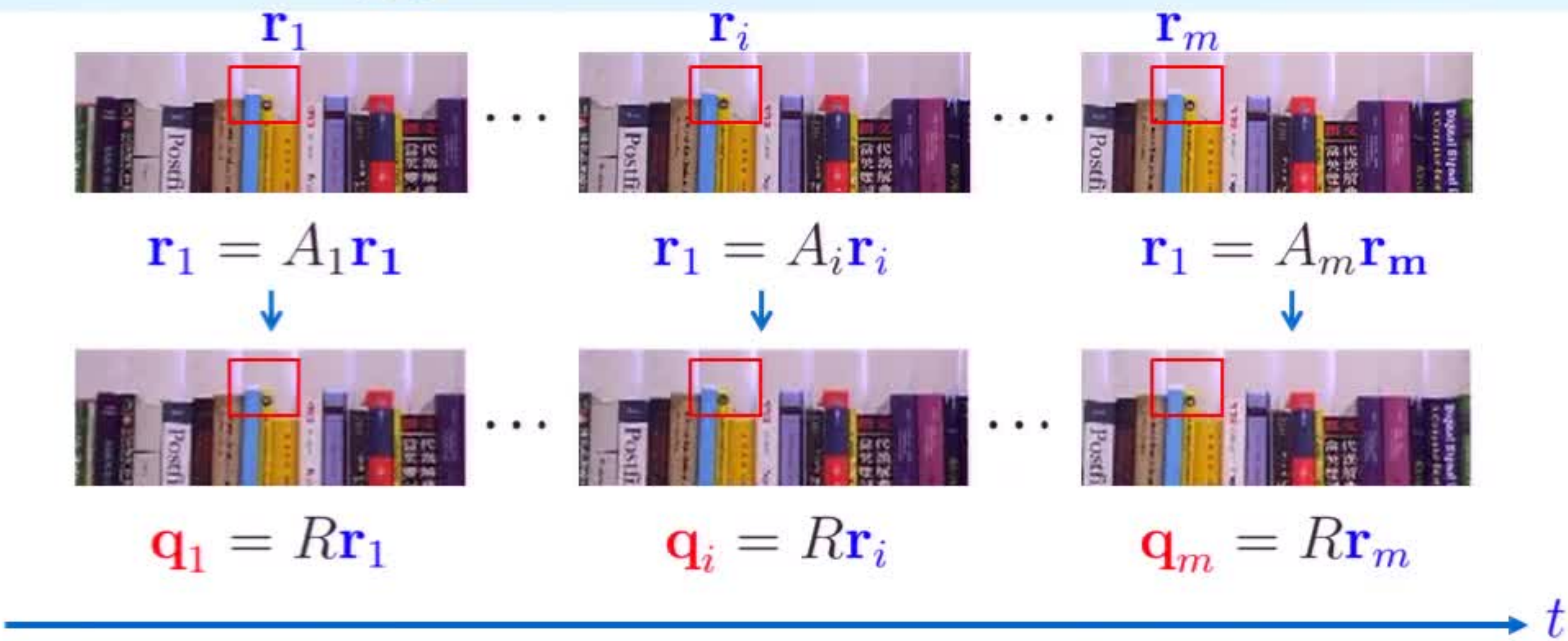

- $\mathbf{q}_i = R\mathbf{r}_i + \mathbf{n}_i, i = 1, \ldots, m.$
- $[A_1\mathbf{r}_1, \ldots, A_m\mathbf{r}_m]$ low rank, so:

$$\min_{\mathbf{r}_i} \operatorname{rank}[A_1\mathbf{r}_1, \ldots, A_m\mathbf{r}_m] + \frac{\alpha}{2}\sum_{i=1}^{m} \|R\mathbf{r}_i - \mathbf{q}_i\|_2^2.$$

Nuclear Norm [Candes, Recht, 09; Recht, Fazel, Parrilo, 10]

$$\min_{\mathbf{r}_i} \|[A_1\mathbf{r}_1, \ldots, A_m\mathbf{r}_m]\|_* + \frac{\alpha}{2}\sum_{i=1}^{m} \|R\mathbf{r}_i - \mathbf{q}_i\|_2^2.$$

- Nuclear norm: $\|U\|_* = \sum_j \sigma_j(U) = \|\boldsymbol{\sigma}(U)\|_1$.
- An ℓ^1-ℓ^2 model. Can be solved by ADMM:
  - Auxiliary variables: $\mathbf{v}_i = A_i\mathbf{r}_i$.
  - $\mathbf{r}_i$-subproblem: $(\alpha R^t R + \beta A_i^t A_i)\,\mathbf{r}_i{}^{j+1} = \mathbf{b}^j$.
  - $\mathbf{v}_i$-subproblem: $[\mathbf{v}_1{}^{j+1}, \ldots, \mathbf{v}_m{}^{j+1}] = \mathrm{SVS}_{\frac{1}{\beta}}(U^j)$.

Comparison

Single frame with bilinear interpolation

Comparison

Single frame with bilinear interpolation

21 frames with nuclear norm

21 frames with TV regularization

21 frames with tightframe approach

HS Image Reconstruction by Tightframe

- Not classical approach:

$$\min_{\mathbf{r}} \|\mathcal{T}\mathbf{r}\|_1 + \frac{\alpha}{2}\sum_{i=1}^{m} \|RA_i\mathbf{r} - \mathbf{q}_i\|_2^2.$$

- Tightframes are generalization of wavelets. Explain idea by the simplest tightframe, the Haar wavelet.

- Consider the simplest case: 4 low-resolution images merge into 1 high-resolution image:

HS Image Reconstruction by Tightframe

- Not classical approach:

$$\min_{\mathbf{r}} \|\mathcal{T}\mathbf{r}\|_1 + \frac{\alpha}{2}\sum_{i=1}^{m} \|RA_i\mathbf{r} - \mathbf{q}_i\|_2^2.$$

- Tightframes are generalization of wavelets. Explain idea by the simplest tightframe, the Haar wavelet.

- Consider the simplest case: 4 low-resolution images merge into 1 high-resolution image:

LR images $\mathbf{q}$ align exactly at half-pixel

High-resolution $\mathbf{p}$

The Process from HR to LR

4 perfectly aligned
LR images merge
into 1 HR image:

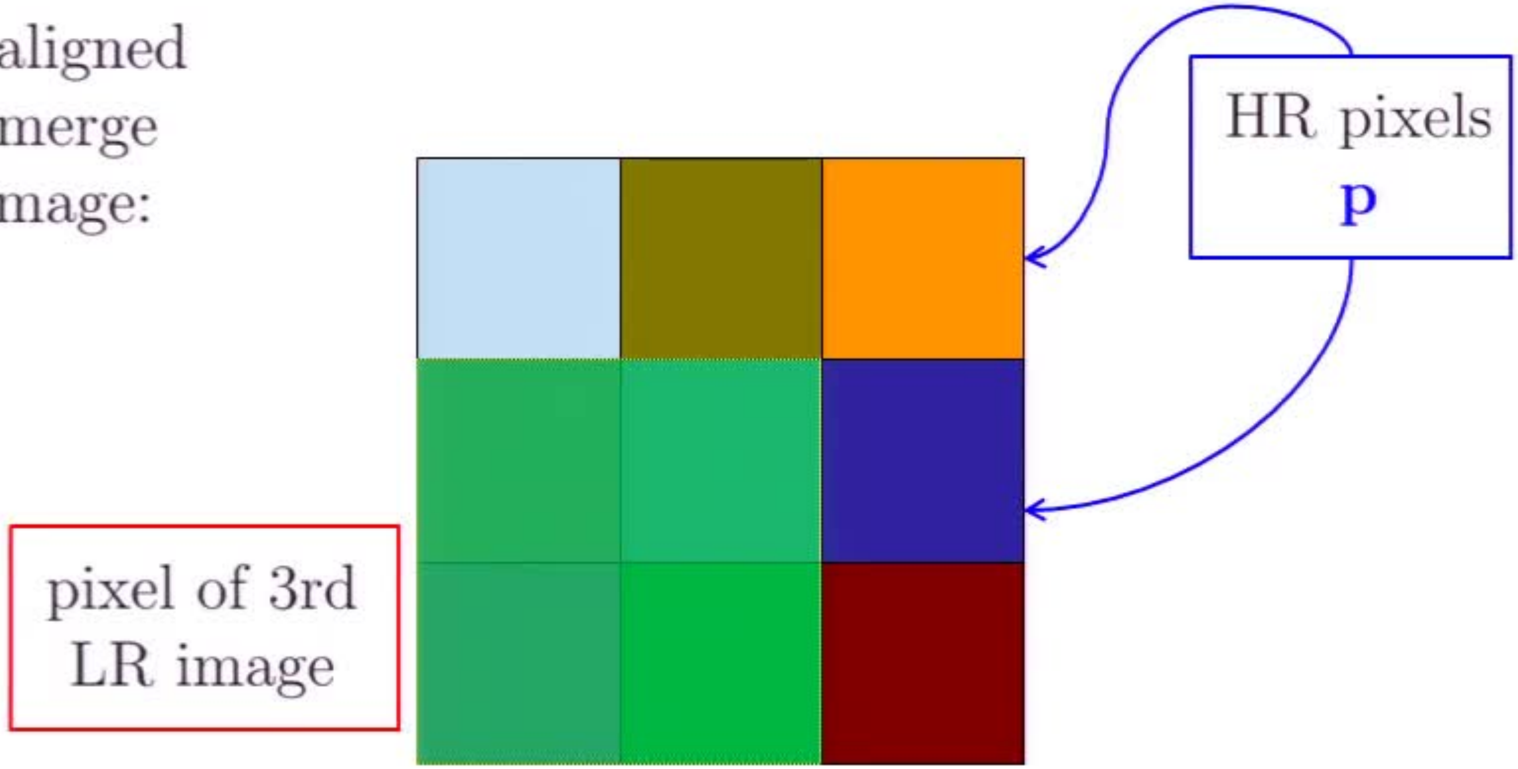

- HR $\to$ LR process = convolution (blurring) with kernel

$$\left(\ldots, 0, \frac{1}{2}, \frac{1}{2}, 0, \ldots\right) \otimes \left(\ldots, 0, \frac{1}{2}, \frac{1}{2}, 0, \ldots\right)$$

- $[\frac{1}{2}, \frac{1}{2}]$ is Haar's low-pass filter

Key Observation

High-resolution **p**

LR images **q** align exactly at half-pixel

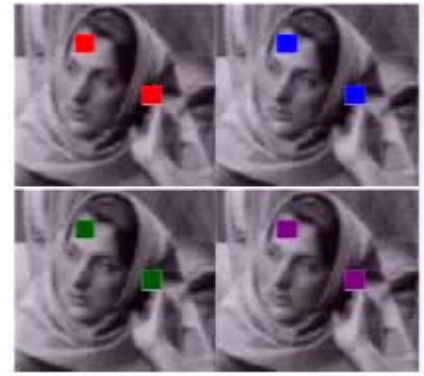

$$\begin{bmatrix} \ddots & \ddots & & & & & \\ & \frac{1}{2} & \frac{1}{2} & & & B & \\ & & \frac{1}{2} & \frac{1}{2} & & & \\ & & & \frac{1}{2} & \frac{1}{2} & & \\ & & & & \frac{1}{2} & \frac{1}{2} & \\ & & & & & \ddots & \ddots \end{bmatrix} \mathbf{p} = \begin{bmatrix} \blacksquare \\ \blacksquare \\ \blacksquare \\ \blacksquare \\ \vdots \\ \blacksquare \\ \blacksquare \\ \vdots \\ \blacksquare \\ \blacksquare \end{bmatrix} \mathbf{q}$$

→ low-pass wavelet coefficients of **p**

- ☐ $B\mathbf{p} = \mathbf{q}$ with B block-Toeplitz-Toeplitz-block.

Frequency Domain Inpainting

HR image reconstruction = frequency domain inpainting

$\mathbf{p}$

$\mathcal{T}$

tightframe transform

Frequency Domain Inpainting

HR image reconstruction = frequency domain inpainting

- ☐ The low-pass framelet coefficients $\mathbf{q}$ are given at locations Γ.
- ☐ Find $\mathbf{p}$ such that $P_\Gamma \mathcal{T}\mathbf{p} = P_\Gamma \mathbf{q}$.

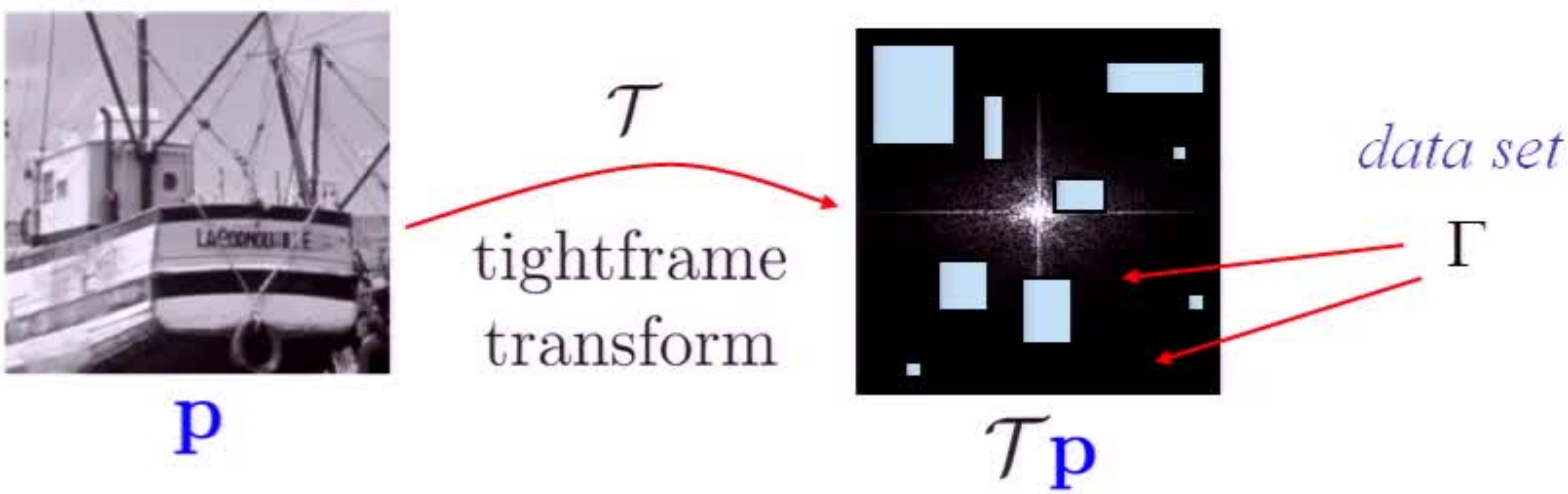

Tightframe Algorithm for Inpainting

For $j = 0, 1, \ldots,$ until convergence:

1. Compute $\mathbf{c}^j = \mathcal{T}\mathbf{p}^j$.

2. Data fitting: set

$$[\mathbf{c}_d^j]_l = \begin{cases} [\mathbf{q}]_l, & l \in \Gamma \\ [\mathbf{c}^j]_l, & l \notin \Gamma. \end{cases}$$

3. Denoise $\mathbf{c}_d^j$ by shrinkage to get $\mathbf{c}_t^j$.

4. Reconstruct $\mathbf{p}^{j+1} = \mathcal{T}^t \mathbf{c}_t^j$.

Note that for tightframes, we have $\mathcal{T}^t\mathcal{T} = I$.

Tightframe Algorithm for Inpainting

The tight-frame frequency domain inpainting algorithm:

$$\mathbf{p}^{j+1} = \mathcal{T}^t \mathcal{S}_\lambda \big(P_{\Gamma^c} \mathcal{T} \mathbf{p}^j + P_\Gamma \mathbf{q} \big)$$

where

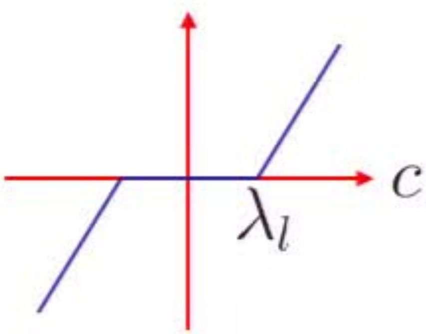

- P_{Γ^c}: projection onto complement of Γ
- $\mathcal{S}_\lambda$: shrinkage operator with threshold $\boldsymbol{\lambda}$

$$s_{\lambda_l}(c) \equiv \begin{cases} \text{sgn}(c)(|c| - \lambda_l), & \text{if } |c| > \lambda_l, \\ 0, & \text{if } |c| \le \lambda_l. \end{cases}$$

16-to-1
sensor
array

16 LR images

16-to-1
sensor
array

16 LR images

recovered

Piecewise linear tightframe is used in our examples.

16-to-1
sensor
array

16 LR images

recovered

only
4 LR
images
given

4 LR images

recovered

Piecewise linear tightframe is used in our examples.

Iterative Thresholding Algorithms

- $[C^2 + S^2$, SISC, 03]:
  Proximal forward-backward algorithm
- [Daubechies, Defrise, & De Mol, CPAM 04]
  Iterative thresholding with sparsity constraint
- [Elad, Starck, Querre & Donoho, MCA 05]
  Simultaneous cartoon and texture image inpainting
- [Combettes & Wajs, SIAM MMS, 05]
  Signal recovery by proximal forward-backward splitting
- [Beck & Teboulle, SIIMS 09]
  A fast iterative shrinkage-thresholding algorithm (FISTA)
- ...

Inpainting in Image Domain

Find image $\mathbf{p}$ from data $\mathbf{q}$ given on Λ, i.e $\mathcal{P}_\Lambda \mathbf{p} = \mathcal{P}_\Lambda \mathbf{q}$.

$$\mathbf{p}^{j+1} = \mathcal{P}_{\Lambda^c} \mathcal{T}^t \mathcal{S}_\lambda \mathcal{T} \mathbf{p}^j + \mathcal{P}_\Lambda \mathbf{q}$$

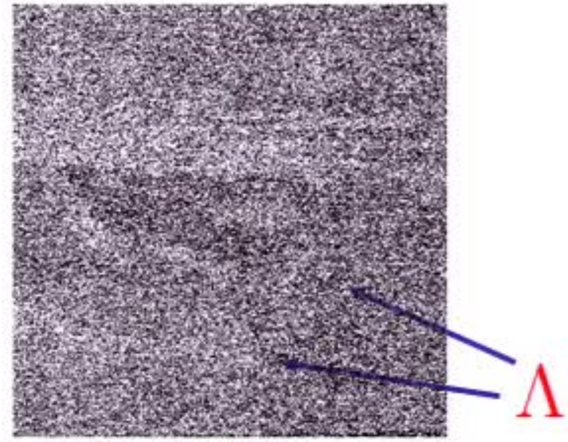

70% S+P noise

Inpainting in Image Domain

Find image $\mathbf{p}$ from data $\mathbf{q}$ given on Λ, i.e $\mathcal{P}_\Lambda \mathbf{p} = \mathcal{P}_\Lambda \mathbf{q}$.

$$\mathbf{p}^{j+1} = \mathcal{P}_{\Lambda^c} \mathcal{T}^t \mathcal{S}_\lambda \mathcal{T} \mathbf{p}^j + \mathcal{P}_\Lambda \mathbf{q}$$

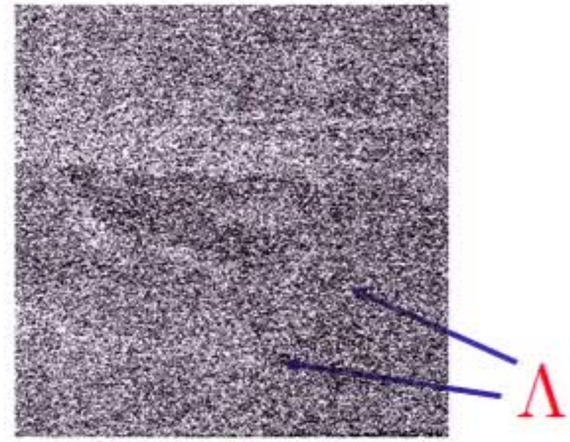

70% S+P noise

Adapative Median Filter
(AMF)

Inpainting in Image Domain

Find image $\mathbf{p}$ from data $\mathbf{q}$ given on Λ, i.e $\mathcal{P}_\Lambda \mathbf{p} = \mathcal{P}_\Lambda \mathbf{q}$.

$$\mathbf{p}^{j+1} = \mathcal{P}_{\Lambda^c} \mathcal{T}^t \mathcal{S}_\lambda \mathcal{T} \mathbf{p}^j + \mathcal{P}_\Lambda \mathbf{q}$$

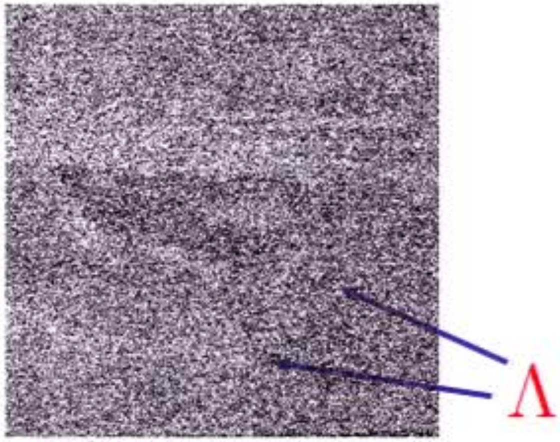

70% S+P noise

Adapative Median Filter (AMF)

AMF + ℓ^1-ℓ^1

[C., Ho, Nikolova, 05]

Inpainting in Image Domain

Find image $\mathbf{p}$ from data $\mathbf{q}$ given on Λ, i.e $\mathcal{P}_\Lambda \mathbf{p} = \mathcal{P}_\Lambda \mathbf{q}$.

$$\mathbf{p}^{j+1} = \mathcal{P}_{\Lambda^c} \mathcal{T}^t \mathcal{S}_\lambda \mathcal{T} \mathbf{p}^j + \mathcal{P}_\Lambda \mathbf{q}$$

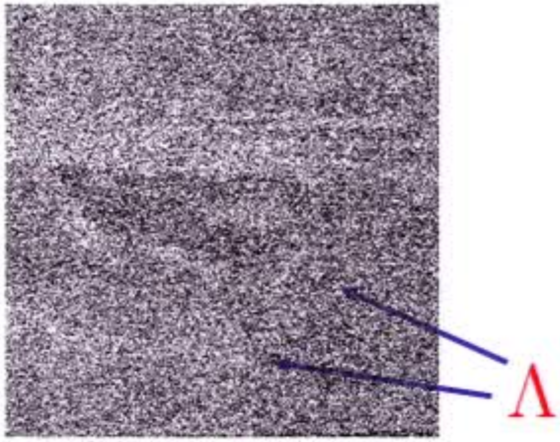

70% S+P noise

Adapative Median Filter (AMF)

AMF + ℓ^1-ℓ^1 [C., Ho, Nikolova, 05]

AMF + tightframe [Cai, C., Shen, Shen, 09]

Single Frame Upsampling

HR video from
LR video

Single Frame Upsampling

HR video from
LR video

Single Frame Upsampling

HR video from
LR video

interpolate/inpaint

Input Video

Qian *et al.* Siggraph 09: $\|\Psi(\nabla \mathbf{f})\|_1$

Upsampled by bicubic

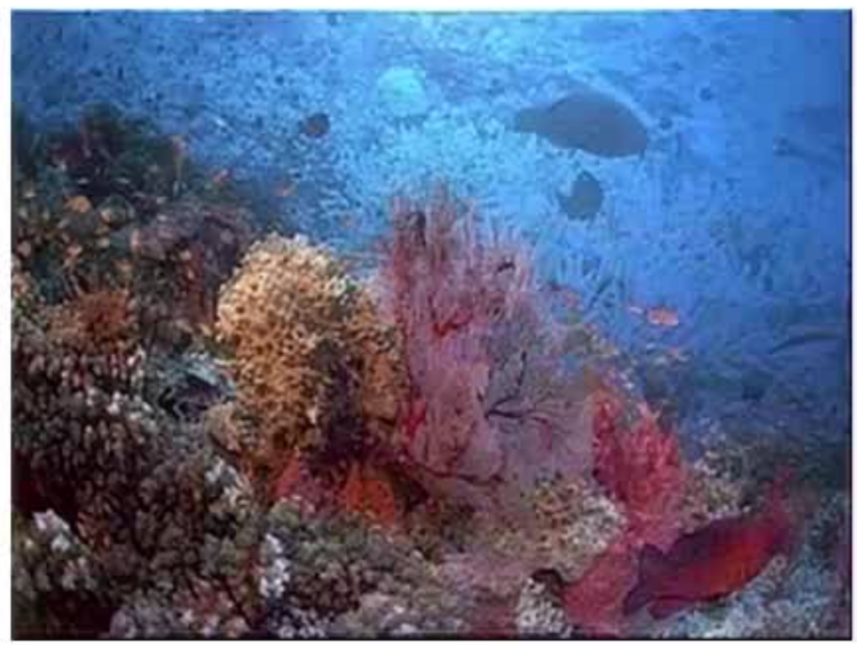

Level 6 Tightframe

Input Video

Qian *et al.* Siggraph 09: $\|\Psi(\nabla \mathbf{f})\|_1$

Upsampled by bicubic

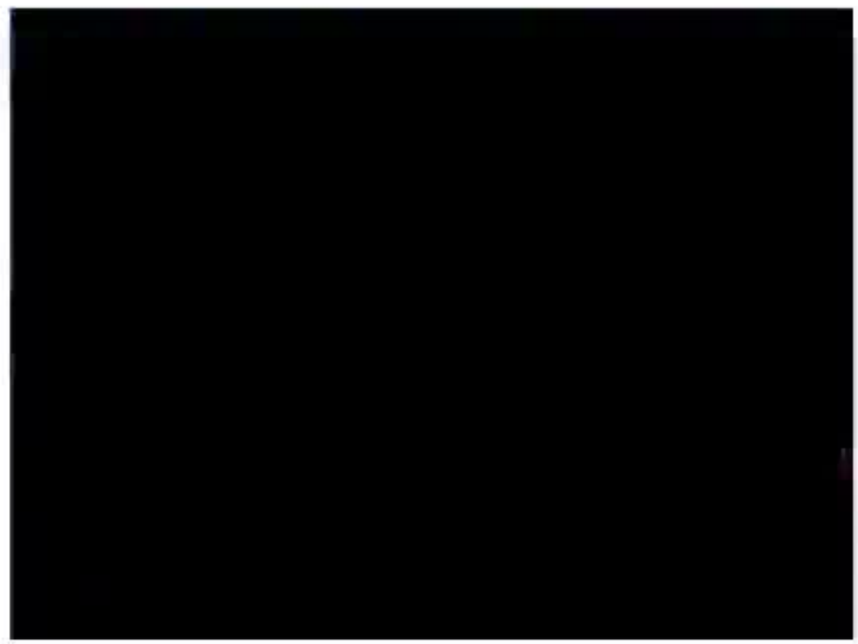

Level 6 Tightframe

Thanks to the Collaborators

- Jianfeng Cai (HK University of Science & Technology)
- Tony Chan (HK University of Science & Technology)
- Mila Nikolova (ENS Cachan)
- Lixin Shen (Syracuse University)
- Zuowei Shen (National University of Singapore)
- Xiaoming Yuan (HK Baptist University)
- Wenxing Zhang (China Uni. of Electronic Science & Tech.)

Thank you for your attention!

Welcome to SIAM LA18 in Hong Kong

May 4-8, 2018

Welcome to SIAM LA18 in Hong Kong

May 4-8, 2018

Welcome to SIAM LA18 in Hong Kong

May 4-8, 2018

Concluding Remarks

- ℓ^1-ℓ^2 problems are common in image processing
- Efficient solvers by adding auxiliary variables
- Solution requires solving a linear system for every outer iteration
- Some requires computing an SVD for every outer iteration

Input Video

Qian *et al.* Siggraph 09: $\|\Psi(\nabla \mathbf{f})\|_1$

Upsampled by bicubic

Level 6 Tightframe